Research article

Microwave absorber utilization to improve grinding and particle surface structure characteristics of torrefied switchgrass particles for bioenergy applications

Obiora S. Agu [a], Lope G. Tabil [a,*], Edmund Mupondwa [a,b], Bagher Emadi [a]

[a] *Department of Chemical and Biological Engineering, University of Saskatchewan, 57 Campus Drive, Saskatoon, SK, S7N 5A9, Canada*
[b] *Bioproducts and Bioprocesses, Science and Technology Branch, Agriculture and Agri-Food Canada, Government of Canada, Saskatoon Research and Development Center, 107 Science Place, Saskatoon, SK, S7N 0X2, Canada*

A B S T R A C T

Torrefaction treatment improves biomass grindability by transforming the fibrous herbaceous to a more brittle and lighter coal-like material. Microwave-assisted torrefaction is a promising technology for biomass conversion into energy, fuels, and chemicals. The study applied microwave absorbers in the torrefaction process to improve the thermochemical characteristics and grindability of switchgrass. Switchgrass in two particle sizes was torrefied in a microwave reactor with biochar added as a microwave absorber under inert conditions. After torrefaction, the geometric mean particle and size distribution and selected physical characteristics were evaluated, and the grindability of the torrefied ground and chopped with and without biochar were compared with those of untreated switchgrass. The geometric diameter results decreased, and the specific energy required for grinding torrefied switchgrass with biochar was significantly reduced with extended residence times and at a torrefaction temperature of 300 °C. After grinding, the lowest grinding energy of 32.82 kJ at 300 °C/20 min was recorded with torrefied ground switchgrass/biochar. The 10% biochar added/250 °C resulted in deep cell wall disarrangement, whereas at a torrefaction temperature of 300 °C, large surface deformation and carbonized weight fractions were observed.

1. Introduction

Sustainable energy innovations bring a shift from centralized fossil fuel-based energy to new energy innovation systems through advanced policies and low carbon emissions sustainability. Using agricultural waste for energy is essential in reducing dependence on fossil fuels. Over the past two decades, there has been a significant global effort to increase the utilization of renewable energy sources from agricultural residues for combined power generation and heat production, representing a huge opportunity for enhancing the bioeconomy sector. Fossil resource utilization and greenhouse gas emissions (GHGs) challenges have enhanced the use of biomass as an energy source and reducing carbon-dioxide emissions, converting lignocellulosic biomass into liquid fuels or gas via pyrolysis, gasification, and anaerobic digestion [1,2]. Besides the environmental advantages in reducing the impact of burning fossil fuels, energy transition using biomass is not limited to engineering, technological innovations, and bioeconomy, thus including physical and social

---

geographies and meanings within the deployed locations [3–5].

Zheng and Qiu [6] study highlighted that Saskatchewan, Canada, has available varieties of biomass for potential usage in biofuel and bioenergy industries, which produce various by-products and have continued to generate revenue in the bioeconomy. The focus is on agricultural crop residues such as switchgrass, camelina straw, oat straw, barley straw, wheat straw, and canola straw. Switchgrass (*Panicum virgatum* L.) is a herbaceous perennial grass that originated in the prairies of central North America and is predominantly grown in eastern Canada, especially Ontario and Quebec [7]. Switchgrass is a dedicated energy crop for bioenergy applications, bio-fibre, livestock bedding, valuable soil protection cover crops, and wildlife habitats. The switchgrass market in Canada is ahead of the United States in developing biofuel pellets. The cultivation is done on millions of acres that cannot support food crop production. Extensive research in converting switchgrass to bioethanol and fuel pellets has shown significant successful results for utilization in bioenergy industries [6,8].

Lignocellulosic biomass has undergone a series of commercial achievements; first-generation feedstocks have shown successful results in biofuel production, whereas second- and third-generation feedstocks are still in research and development stages alongside techno-economic evaluations and life cycle assessments [9,10]. Several studies have reported that the torrefaction process at a temperature of 250–300 °C has improved physical, mechanical and fuel characteristics comparable to coal [4,11]. Thus, successful results have been recorded highlighting interparticle improvement in biomass grinding performance for energy utilization and vary with the type of biomass used [12]. Many research investigations have compared the results of conventional and microwave torrefaction processes, highlighting their advantages and disadvantages. Microwave heating is from the inside of the biomass via wave interactions, while conventional heating is from the surface to the center of the material. However, microwave torrefaction efficiency has shown enhanced product yield and reduced energy consumption compared to conventional torrefaction processes [13,14]. Also, advantages of the microwave torrefaction process include precise and controlled heating, faster heat transfer than conventional, environmental friendliness, and potential economic benefits over traditional heating [15–17]. Several studies on microwave torrefaction have highlighted its efficiency at the pilot scale on product yield conversions and possible industrial scaling up for producing quality plant material extracts [18,19].

A microwave absorber enhances heat absorption rate and speeds up interparticle reactions during torrefaction. Also, the microwave absorber increases the torrefaction temperature at reduced microwave power and improves volumetric heating with good penetration depth [20,21]. Agricultural residues, forestry and non-agricultural materials have been identified as good microwave absorbers and applied in the torrefaction process. In addition, microwave absorbers have shown successful utilization, improving solid yield quality, heat irradiation particle interactions and after-use environmental friendliness [19]. Overall, the torrefaction treatment techniques developed two decades ago have been to commercialize the process and conduct techno-economic assessments and life cycle analysis in choosing sustainable processes [22,23]. Notably, torrefied biomass in a pulverized coal-fired plant must describe fuel properties before utilization. Also, co-firing with natural/raw biomass could lead to incomplete combustion, like having particle size distribution of ground biomass larger in size and different from coal, causing lower burn-out efficiencies [11].

Grinding to desired particle size requires high-energy input, and finely ground biomass is compulsory in fuel boilers or gasifiers [24]. According to Mani et al. [25], grinding biomass with high moisture content involves higher specific energy consumption. Many studies reported that the energy needed for grinding biomass depends on the physical properties, biomass compositions, and grinding characteristics [26,27]. Torrefaction at mild and severe conditions improves biomass grinding. It enhances other physicochemical properties such as hydrophobicity, resistance to fungal and microbial degradation and decomposition, leaving the biomass more brittle and friable compared to raw biomass [12,26]. Biomass is tenacious, while some are fibrous, and torrefaction conditions make biomass loss toughness, breaking down the hemicellulose matrix and depolymerizing cellulose. To an extent, the severity of the process conditions has shown good grinding performance and energy savings during grinding [28,29]. Therefore, microwave torrefaction can treat switchgrass and increase the energy density of the biofuel pellet for industrial utilization.

As anticipated, investigations are ongoing to evaluate the solid yield from torrefied biomass with microwave absorbers for biorefinery utilization (standard fuel particle analysis and energy yield). So far, few studies reported improving the grindability properties [18,20,30,31]. Also, few research studies have examined the extent of cell-wall breakdown after torrefaction treatment and the mass yield's physical and chemical characteristics [31]. Thermal pretreatments such as microwave torrefaction influence shrinkage and grindability, thus showcasing the interparticle structures of the biomass. The microparticle transformation study reveals structural features and particle changes, which are examined using microscopy techniques such as scanning electron microscope (SEM) and confocal laser scanning microscopy (CLSM) [2,32,33]. SEM and CLSM are applied to further study and evaluate the significant effect of microwave torrefaction on the surface morphology of torrefied biomass. The CLSM technique has microscopy advantages over SEM, such as in fluorescence intensity and revealing fluorescence channels in all dimensions, two- or three-dimensional (2D or 3D) scanning to detect multiple channels simultaneously, separating polarized and scattered light [34,35]. Furthermore, CLSM has a higher intensity of film-core interface, which provides detailed interface characterization and difference in particle's fluorescence intensity, represents a non-destructive technique and gives in-depth, measurable information on the thickness and surface composition of pellets than SEM [33]. The microscopy technique generates planar vertical or horizontal sections using 2D or 3D software maps to interpret multiple channel distributions. There is a lack of knowledge in utilizing the CLSM technique to characterize or examine the solid fuel properties of thermochemical converted biomass. Furthermore, many research studies have used CLSM techniques in biomedical, material sciences, geosciences, and agricultural investigations and reported successful image results [32,36].

Consequently, the study is a continuation of the effect of biochar addition in microwave torrefaction of switchgrass torrefaction, as previously reported [37]. The hypothesis is that using microwave torrefaction conditions with a microwave absorber could enhance torrefied biomass grinding performance. In addition, there is a knowledge gap in evaluating the effect of particle size on microwave torrefied biomass with microwave absorbers. For sustainable scaling up of the process, raw or torrefied biomass grinding

characteristics are needed to select and design grinding equipment for bioenergy applications [27]. The study aimed to determine the effect of microwave torrefaction conditions on grinding energy, examining the surface physiological changes of torrefied ground or chopped switchgrass particles by evaluating distinct microparticle changes with and without biochar using a confocal laser scanning microscope.

2. Materials and method

2.1. Materials

Switchgrass (SG) of the variety "Cave-in-rock" was harvested from a farm in Nappan, Nova Scotia, Canada. The untreated SG received was subjected to two modes of particle size reduction: ground and chopped. The hammer mill (Serial no. 6M13688; Glen Mills Inc., Maywood, NJ, USA) was used to ground SG (screen size of 6.4 mm), while the chopped SG (manually reduced using 25–50 mm size) equivalent to the tub grinder output [25], and the biochar (microwave absorber) from Soil-matrix, Air Terra, Calgary, AB, Canada. The properties of as-received SG and biochar are presented in Table 1, summarizing the thermochemical analysis and compared with coal before the microwave torrefaction treatment. The proximate and elemental analysis values are important for utilization in bioenergy. As observed, the moisture contents of raw SG and biochar showed comparatively high moisture content, which is a desirable characteristic in the initial microwave absorption. Also, there is low ash content, potentially higher calorific values, and better heating rates than coal. Coal ash content is approximately six times more than SG and approximately twice that of biochar. It shows that fractions of SG and biochar have combustion and heat properties that can provide stable fuel with possible combustion unit challenges and potential environmental friendliness. The SG (ground or chopped) with biochar mix was stored in air-tight Ziploc bags for further analysis experiments.

2.2. Microwave torrefaction experimental setup

The microwave (2.45 GHz, LBM 1.2A/7296, Cober Electronics Inc., Stamford, CT, USA) torrefaction heating treatment was carried out in a custom cylindrical quartz reactor and was conducted in triplicates (Fig. 1). A thermocouple covered with Teflon was inserted in the middle port to measure the heat distribution in the reactor; and the data was recorded with real-time graphing and data logging software (OSENSA Innovation Corp. Coquitlam, BC, Canada).

A biomass-biochar mixture of $\approx 100 \pm 0.02$ g was placed in the reactor for each experiment stage of ground or chopped SG, and the heating treat done separately. The microwave was turned off at 520 W or 650 W once the temperature of 250 °C or 300 °C and corresponding residence times (10, 15, or 20 min) were attained. The mass yield fraction was allowed to cool at room temperature and kept for further analysis, and the torrefaction severity was determined using equation (1) [38].

$$\text{Degree of torrefaction, DT} = 1 - \frac{\text{VM}_{ts}}{\text{VM}_{uts}} \tag{1}$$

where DT = degree torrefaction, VM_{ts} and VM_{uts} are the volatile matter of the torrefied and untorrefied samples.

2.3. Torrefied switchgrass particle size characterization

2.3.1. Particle density and bulk density

Torrefied SG with and without biochar and raw SG particle and bulk density were determined using a gas displacement pycnometer (AccuPyc 1340, Micromeritics Instruments Corp., Norcross, GA, USA) at 24 ± 0.7 °C to measure particle density. Bulk density was measured and evaluated by the mass and volume of a standard cylindrical steel container with 0.5 L (SWA951, Superior Scale Co. Ltd., Winnipeg, MB, Canada), having the sample filled the cylindrical container and applying a steady rolling pattern across with no pressure exerted on the sample. The sample weight was determined and replicated seven times for raw and torrefied SG.

Table 1
Physico-chemical characterization of untreated switchgrass, biochar and coal.

Parameters	Switchgrass	Biochar	Coal[b]
Moisture content (% w.b.)	9.10	15.35	29.18
Ash (% d.b.)	2.67	7.67	15.20
Volatile matter (wt. % d.b.)	76.96	49.83	33.06
Fixed carbon (% d.b.)[a]	20.37	42.50	51.74
Bulk density (kg/m³)	91.07	209.53	-
Carbon (%)	46.21	79.81	47.72
Hydrogen (%)	5.95	4.39	1.83
Nitrogen (%)	0.38	0.44	0.92
Sulphur (%)	0.08	0.04	15.06
Oxygen (%)	47.39	15.32	34.47
High heating value (MJ/kg)	18.19	32.89	16.43

w.b.: wet basis; d.b.: dry basis; a: calculated by the difference; b data from Iroba et al. [24].
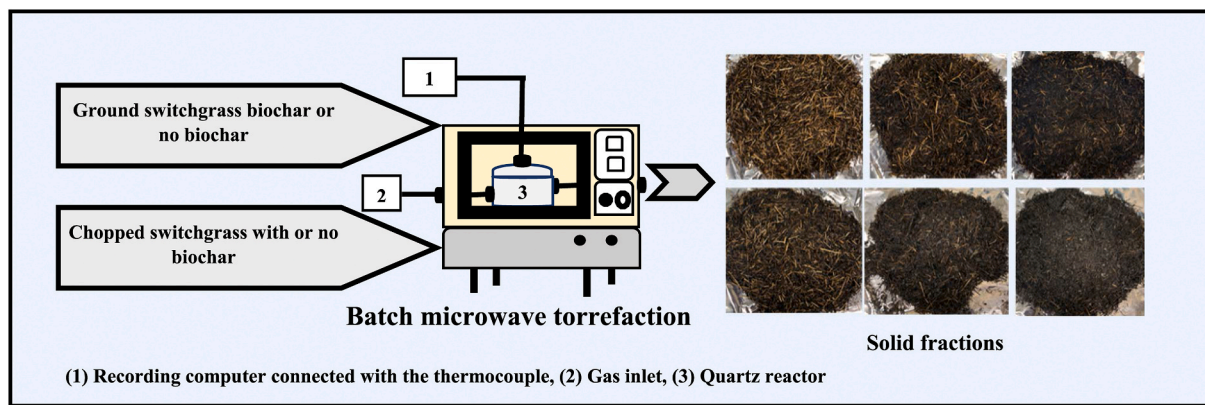
Fig. 1. Bench-top microwave torrefaction setup.

2.3.2. Torrefied switchgrass with and without biochar particle size analysis

The chopped forage size analyzer (ASAE Standard S424.1) was applied for the chopped size of raw SG to evaluate the geometric mean. The ASABE/ASAE S319.4 (R2012) was used for the ground SG particle size analysis [25]. Torrefied ground or chopped SG particle size distribution was determined based on ASABE standard ANSI/ASAE S319.4 (R2012) [25] and replicated three times. The retained mass was weighed and evaluated accordingly (particle distribution, geometric mean diameter, and geometric standard deviation).

2.3.3. Torrefied switchgrass with and without biochar grindability

The microwave torrefied ground or chopped SG with and without biochar grinding characteristics were evaluated using a cutting knife mill (Model N0. 3690604, Dietz-Motoren GmbH & Co. KG, Dettingen Teck, Germany) with a screen size of 3 mm. The grinding trial experiment used ≈50 ± 0.05 g and hand-fed into a mill chute. The power consumption during grinding was recorded with real-time channel software (ELOG 13 ELITEpro XC version ES400.235); immediately, the sample made contact with the knife and stopped when no material came out through the collecting chute. The process was replicated three times to check the reproducibility of the experiment, and after, the grinding energy was determined as the product of the grinding time, the average current drawn during the process and the voltage, considering the mass quantity fed into the chute.

2.4. Microscopy examinations

The untreated ground or chopped SG and torrefied ground or chopped SG with and without biochar surface analysis were examined using CLSM (LSM 880 with AxioObserver, Carl Zeiss Microscopy LLC, White Plains, NY, USA) in a 10x magnifying lens (x:425.10/y: 425.10 tiles). Since dried samples were used, the excitation and emission wavelengths were set at 405 μm and 484 μm, respectively [39]. Due to the severity of the torrefaction, the degree of heat distortion and biomass structure damage was examined, and the ZEN 3.5 Lite 2.5D display (Carl Zeiss Microscopy, LLC, White Plains, NY, USA) was used to study and evaluate the patterns of surface structural opening after torrefaction. The fluorescence spectroscopy intensities, such as sum and mean fluorescence intensity, were analyzed automatically using ZEN lite software. In addition, the heat distortion depth was calculated, and the penetration patterns were evaluated using ZEN lite 2.5D display and histogram.

2.5. Experimental plan

The statistical analysis is a collection of mathematical and statistical techniques using the design of experiments building models, and evaluating effects of independent factors applied using analysis of variance for response variables (solid yield, moisture content, ash content, geometric mean diameter, bulk and particle densities), and optimizing the process. The torrefied ground or chopped SG with and without biochar grinding characteristics were determined, including the geometric mean diameter and interaction effects of added biochar with residence time at torrefaction temperatures 250 °C and 300 °C analyzed using response surface methodology-user-defined design (UDD) of the Minitab software (Version 20.3; eBase Solutions Inc., Vaughan, ON, Canada).

3. Results and discussion

3.1. Microwave torrefaction of switchgrass and product yields

Table 2 shows the solid fraction yields and physical characteristics between raw SG and torrefied ground or chopped SG with and without biochar at different torrefaction conditions. The biochar addition in torrefied fractions (ground or chopped) obtained was visually observed as uniformly heated, and samples without microwave absorbers revealed that SG was unable to receive heat

Table 2

Effect of torrefaction conditions on mass yield and physical properties between torrefied ground and chopped switchgrass.

| Sample	Torrefaction temperature (°C)	Residence time (min)	Solid yield (%)		Moisture content (% d.b.)		Ash content (% d.b.)		Mass loss (%)		Degree of torrefaction		Bulk density (kg/m³)		Particle density (kg/m³)	
			SG	SG-C	SG	SG-C	SG	SG-C	SG	SG-C	SG	SG-C	SG	SG-C	SG	SG-C
Untreated switchgrass					9.10		2.67						91.07	23.48	1039.8	1007.20
TS-n-B	250 °C	10	71.50	78.18	1.36	1.45	3.09	2.93	28.50	21.82	0.03	0.04	106.80	55.40	1069.50	953.80
		15	69.48	76.83	1.22	1.33	3.50	3.01	30.52	23.17	0.06	0.07	109.40	60.50	1074.40	1009.00
		20	65.68	69.05	1.12	1.27	3.65	3.47	34.32	30.95	0.10	0.11	116.40	63.60	1078.30	1015.10
TS-90/10		10	63.68	65.00	2.01	2.23	3.41	3.43	36.32	35.00	0.11	0.10	167.13	109.50	1107.80	1024.80
		15	57.45	58.70	1.99	2.17	4.48	4.80	42.55	41.30	0.17	0.18	171.07	112.10	1173.20	1026.90
		20	48.48	55.20	1.76	1.95	5.12	5.42	51.52	44.80	0.22	0.20	175.27	117.50	1178.20	1032.60
TS-80/20		10	61.00	62.83	1.82	2.03	4.26	5.15	39.00	37.17	0.16	0.14	180.67	126.70	1225.70	1054.90
		15	55.08	55.73	1.79	1.84	4.60	5.67	44.92	44.27	0.20	0.19	189.00	136.60	1248.50	1089.70
		20	47.25	49.63	1.68	1.51	5.62	6.52	52.75	50.37	0.26	0.21	195.53	140.90	1387.20	1129.60
TS-n-B	300 °C	10	70.36	75.98	1.25	1.36	3.57	3.54	29.64	24.02	0.08	0.09	117.60	60.80	1085.60	983.90
		15	64.80	70.95	1.17	1.21	3.80	3.71	35.20	29.05	0.10	0.10	120.90	69.70	1087.90	1013.80
		20	60.17	64.25	1.09	1.15	3.84	3.99	39.83	35.75	0.14	0.13	123.03	71.20	1103.90	1024.00
TS-90/10		10	55.28	58.08	1.79	1.90	4.35	5.39	44.72	41.92	0.18	0.13	175.93	108.30	1104.00	1043.40
		15	49.03	53.70	1.65	1.78	4.54	5.58	50.97	46.30	0.23	0.21	178.40	116.50	1159.60	1050.60
		20	45.05	49.23	1.35	1.51	4.89	5.65	54.95	50.77	0.31	0.24	182.20	120.00	1215.00	1065.00
TS-80/20		10	53.10	50.70	1.41	1.53	5.51	5.83	46.90	49.30	0.25	0.23	186.07	128.60	1235.00	1082.10
		15	46.03	48.58	1.24	1.37	7.37	6.24	53.97	51.42	0.30	0.27	196.93	140.70	1329.50	1096.00
		20	42.48	45.83	1.19	1.25	7.84	6.63	57.52	54.17	0.36	0.33	207.00	149.50	1374.70	1134.50

SG: switchgrass ground in 6.4 mm sieve; SG-C: chopped switchgrass; TS-n-B: torrefied-switchgrass-no-biochar. The first number after torrefied biomass is % SG and the second is % biochar.

sufficiently. The torrefied SG yield fractions for both grinds decreased between torrefaction temperatures 250 °C and 300 °C/longer residence time. The solid yield declined over half of the original weight at 20 % biochar addition/250 °C/20 min residence time for both grinds and at 10 % biochar addition/300 °C (residence time 15 min for torrefied ground SG with biochar and 20 min for torrefied chopped SG with biochar). However, microwave torrefied SG with and without biochar in both particle sizes showed similar and comparable solid yields. At torrefaction temperatures, 250 °C and 300 °C, the mass loss increased with biochar addition and longer residence times [37]. The mass loss implied that ground SG/biochar reduced hot spots and increased uniform heating compared to chopped SG/biochar. Biochar addition and increased torrefaction temperatures with longer residence times increased the mass loss. On the other hand, mass loss observed in torrefied ground SG was higher than in torrefied chopped SG, and without biochar, mass loss was less than 40 % at both torrefaction temperatures. Moreover, biochar addition contributed to the increase in torrefaction severity, leading to the loss of volatiles.

Furthermore, the decreased particle size of raw SG would increase the bulk and particle densities due to the inter- and intra-particle void reduction as observed during grinding. The bulk density and particle density of torrefied ground or chopped SG with and without biochar increased with the torrefaction conditions, as presented in Table 2. The bulk density increased in torrefied ground or chopped SG with biochar addition/250 °C and 300 °C. Also, the bulk density and particle density values were slightly higher with torrefied ground SG with and without biochar compared to torrefied chopped SG with and without biochar. The biochar fractions-solid yield and corresponding mass loss were significantly affected by adding biochar. However, 300 °C/biochar addition and longer residence times resulted in decreased moisture content and increased ash content compared to the untreated SG. Microwave torrefaction decreases moisture content, resulting in higher energy efficiency, upgrading mass yield quality, and possible emissions reduction [37]. As observed, the increase in the ash content in the torrefied ground or chopped SG with and without biochar compared to the raw SG could be attributed to mass loss.

3.2. Mean particle size and particle size distribution after microwave treatment

The variation in the geometric mean (d_{gw}) particle size of torrefied SG with and without biochar is presented in Fig. 2 (A-C). Compared to the untreated SG (d_{gw}: ground SG 0.579 mm and chopped SG 7.43 mm), the mean particle size of torrefied SG was smaller. The results indicated that increased torrefaction temperature with the addition of biochar and extended residence times

(A)

(B)

(C)
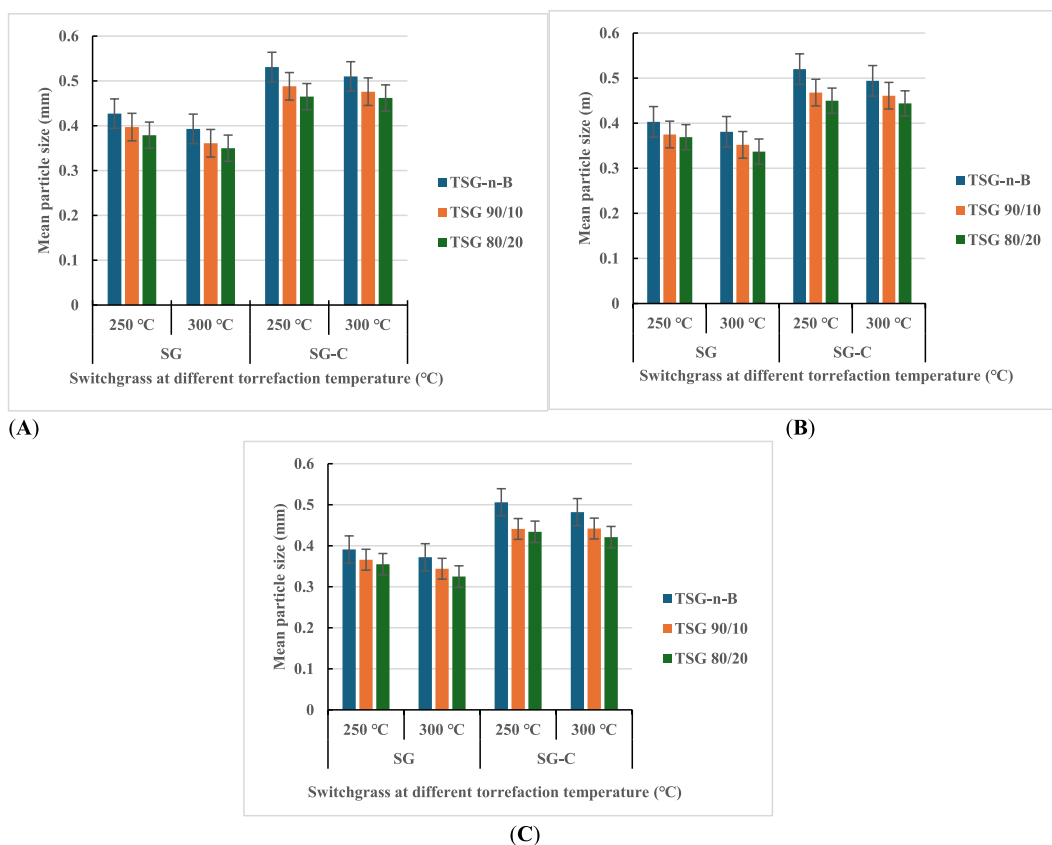
Fig. 2. Mean particle size of ground torrefied switchgrass at different residence times (A) 10 min, (B) 15 min, and (C) 20 min. (SG: switchgrass ground in 6.4 mm sieve; SG-C: chopped switchgrass; TSG-n-B: torrefied-switchgrass-no-biochar. The first number after torrefied biomass is % SG and the second is % biochar.)

Table 3
Mass percentage of torrefied ground and chopped switchgrass as a function of biochar addition, torrefaction temperature, and residence time.

Torrefaction condition			Mass particles retained (%)														
			Screen opening (mm)														
Sample	T T (°C)	RT (min)	1.41		0.84		0.60		0.30		0.21		0.15		Pan	
			SG	SG-C	SG	SG-C	SG	SG-C	SG	SG-C	SG	SG-C	SG	SG-C	SG	SG-C
TS-n-B	250 °C	10	0.20	12.00	19.77	23.21	30.80	24.04	38.41	37.05	8.10	3.40	1.60	0.30	1.10	0.00
		15	0.07	11.63	16.80	21.27	29.40	24.80	39.47	38.37	11.27	3.47	1.70	0.47	1.30	0.00
		20	0.00	10.17	14.70	20.03	29.41	26.20	40.28	39.50	12.30	3.60	1.90	0.50	1.40	0.00
TS-90/10		10	0.03	10.60	13.60	19.70	32.30	25.80	39.73	36.60	10.80	4.10	2.30	1.80	1.20	1.40
		15	0.00	8.40	11.30	18.27	30.07	27.20	40.07	38.50	14.87	4.30	2.40	1.93	1.30	1.40
		20	0.00	6.10	10.40	15.41	28.88	29.51	41.11	40.41	15.50	4.77	2.70	2.00	1.40	1.80
TS-80/20		10	0.00	9.03	10.50	19.03	32.97	24.00	40.10	40.17	12.03	4.40	2.50	1.90	1.90	1.47
		15	0.00	7.80	9.60	16.41	31.50	26.08	41.93	41.81	12.30	4.50	2.47	1.90	2.20	1.50
		20	0.00	6.00	8.30	14.40	29.60	28.40	42.50	42.84	14.40	4.80	2.80	2.00	2.40	1.60
TS-n-B	300 °C	10	0.13	10.30	16.37	22.60	28.07	24.30	40.70	39.20	10.57	2.03	2.30	1.07	1.87	0.50
		15	0.07	9.10	14.20	21.17	28.70	25.60	40.93	40.10	11.40	2.10	2.50	1.10	2.20	0.83
		20	0.00	8.00	12.07	19.90	29.04	26.70	42.11	41.00	11.80	2.20	2.70	1.30	2.27	0.90
TS-90/10		10	0.00	9.10	10.90	18.90	27.40	26.70	41.70	38.30	15.60	3.60	2.40	2.00	2.00	1.40
		15	0.00	8.07	9.40	16.80	27.43	28.10	42.00	39.83	16.30	3.60	2.60	2.10	2.27	1.50
		20	0.00	7.07	7.00	13.30	28.50	30.10	42.40	42.03	16.90	3.70	2.80	2.10	2.40	1.70
TS-80/20		10	0.00	8.97	8.00	17.31	28.03	25.71	43.27	40.71	16.00	3.70	2.60	2.10	2.10	1.50
		15	0.00	7.50	7.70	15.60	24.30	26.60	45.40	42.20	17.50	4.20	2.80	2.20	2.30	1.70
		20	0.00	5.90	5.90	11.37	23.70	29.77	46.10	43.70	18.53	5.07	3.07	2.40	2.70	1.80

SG: switchgrass ground in 6.4 mm sieve; SG-C: chopped switchgrass; TS-n-B: torrefied-switchgrass-no-biochar. The first number after torrefied biomass is % SG and the second is % biochar; TT: torrefaction temperature; RT: residence time.

showed a smaller average particle size of the torrefied ground SG compared to the torrefied chopped SG. Torrefied ground or chopped SG without biochar showed larger mean particle sizes ranging from 0.531 mm to 0.372 mm than torrefied ground or chopped SG with biochar (0.488–0.325 mm). Notably, torrefied SG without biochar indicated larger geometric particle diameters and lower bulk and particle densities. Whereas smaller geometric mean diameters and higher bulk and particle densities were observed with the torrefied SG with biochar (Fig. 2C). It implies that the biochar addition was more effective in the heat absorption rate with ground SG than chopped SG.

Table 3 presents the particle size distribution of torrefied SG with and without biochar added and compared with untreated SG given in Table S1. The result varies after torrefaction in two temperatures, 250 °C and 300 °C, and untreated SG showed differences in particle sizes and mass fractions retained. According to Mani et al. [25], coarse particles adequately feed boilers and gasifiers heat plants. Also, Li et al. [20] highlighted that a microwave absorber mixed with size-reduced biomass has the potential to improve
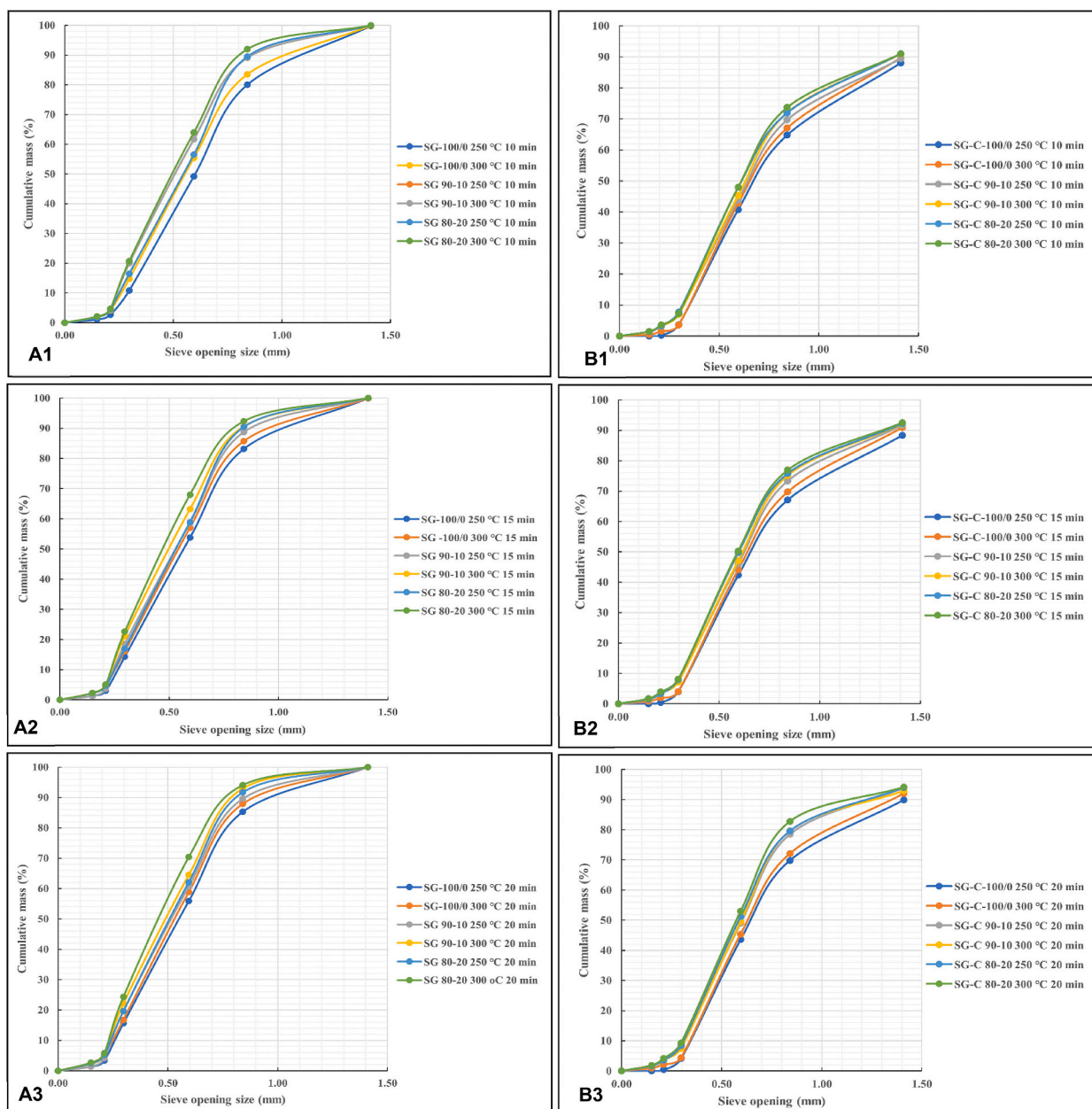
Fig. 3. Cumulative passing plot of particle size between torrefied ground switchgrass (A) and torrefied chopped switchgrass (B) with and without biochar/residence times: A1 and B1 (10 min), A2 and B2 (15 min), and A3 and B3 (20 min) at 250 °C and 300 °C torrefaction temperatures. (SG: switchgrass ground in 6.4 mm sieve; SG-C: chopped switchgrass; TSG-n-B: torrefied-switchgrass-no-biochar. The first number after torrefied biomass is % SG and the second is % of biochar).

uniform heating within the material. The quantities of torrefied SG weight fractions collected in the smaller sieve and pan were more at 300 °C than 250 °C.

The torrefied ground SG/biochar had more particles at the sieve's bottom plate compared to torrefied chopped SG/with biochar. Torrefied ground SG/biochar 20 % at 300 °C/20 min had more fine particles passed the 0.2 mm screen size. Torrefied ground or chopped SG with and without biochar showed little significant changes above 0.3 mm screen size, indicating larger or coarse SG particle sizes. Torrefied ground SG starting with 10% biochar/250 °C showed small particle sizes and fine fractions at 300 °C. The results revealed that torrefied SG with biochar has the potential to improve grinding characteristics irrespective of particle size mode after microwave torrefaction. Thus, increasing from 250 °C to 300 °C reduced the structural size of the torrefied SG for both grinds. The cumulative mass percentage of particle size for untreated SG (Fig. S1) and torrefied SG with and without biochar are presented in Fig. 3. The plots in Fig. 3 (A1-3 and B1-3) showed a similar curve indicating the effects of microwave irradiation before grinding and compared with untreated SG. The cumulative plots with biochar followed a similar curve, and there were overlaps in the particle size range.

The distribution curves of torrefied chopped SG without biochar showed larger particles than the torrefied ground SG without biochar. Torrefied ground SG without biochar showed different curves and uniform particle size ranges compared to torrefied chopped SG without biochar. In addition, the smaller weight fractions consistently increased as reaction temperatures shifted from 250 °C to 300 °C for both grinds, showing the significance of biochar addition (Fig. 3A1 – 3 and 3B1 – 3). Furthermore, ground SG indicated more sensitivity to thermal reaction than chopped SG with biochar addition. The distribution curves showed that torrefied ground SG with biochar retained more samples at the bottom plate than the torrefied chopped SG with biochar. The results implied that the particle size weight fractions after torrefaction can be attributed to the carbonization of biomass particles. The untreated SG generated a wider particle size range compared to the torrefied ground or chopped SG with and without biochar.

3.3. Energy expended in grinding of torrefied biomass

Grinding performance and geometric mean diameter of torrefied SG are presented in Fig. 4. The torrefied ground SG without biochar showed the energy requirement decreased by 69.26% and 68.38% for torrefied chopped SG without biochar at 300 °C (Fig. 4A and B). The results implied that grinding energy consumption depends on torrefaction temperature and feedstock. Improved grinding could be attributed to the loss of volatile components and moisture to the surrounding environment, breaking down hemicellulose at
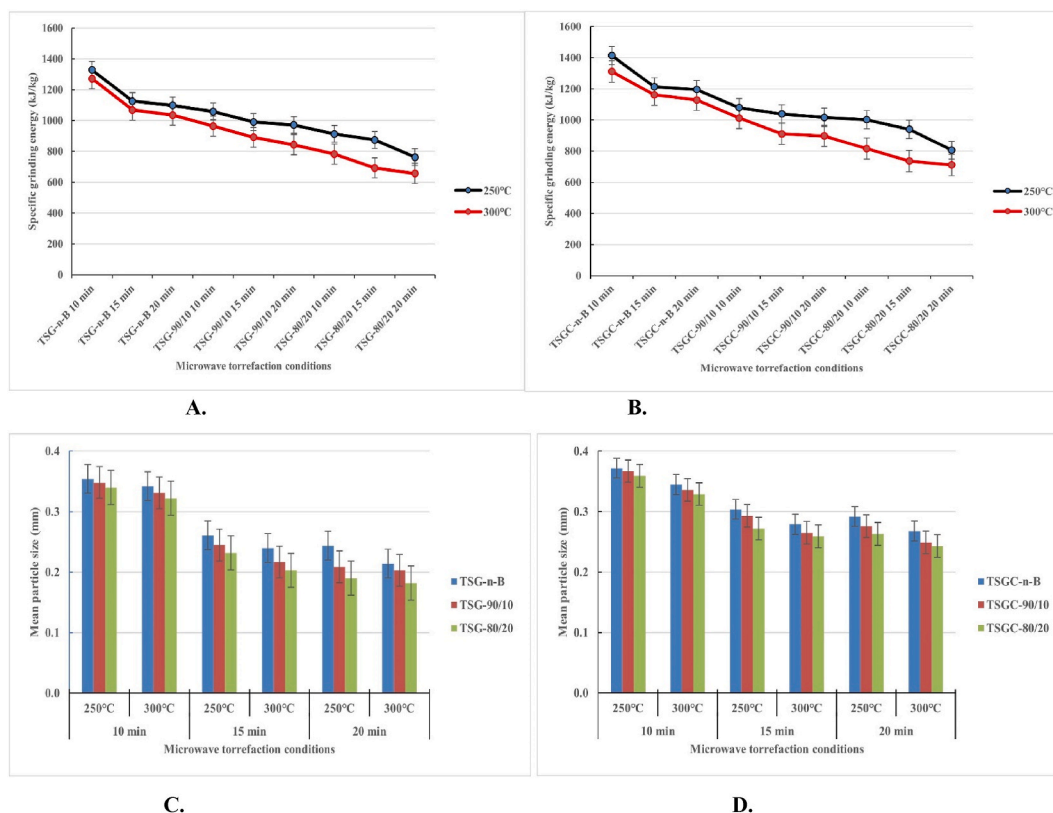
Fig. 4. Effect of torrefaction conditions on specific grinding energy (A,B) and mean particle size (C,D) for ground torrefied ground switchgrass and torrefied chopped switchgrass. (SG: switchgrass ground in 6.4 mm sieve; SG-C: chopped switchgrass; SG-100/0: torrefied-switchgrass-no-biochar. The first number after torrefied biomass is % SG and the second is % of biochar).

250 °C and cellulose and lignin components at > 250 °C and beyond 300 °C, which leaves the torrefied SG mass yield very brittle and carbonized [37]. The effect of microwave torrefaction conditions on the mean particle size of torrefied ground or chopped SG ground through a 3 mm screen size indicated lignocellulosic matrix disintegration made the grinding easier and produced more small particles than the sizes produced after microwave torrefaction. Regardless of the SG particle size reduction method, adding biochar at torrefaction treatment significantly affected the grindability of torrefied ground or chopped SG. The energy requirement decreased by 86.30% for torrefied ground SG and 86.12% for torrefied chopped SG at 300 °C torrefaction temperature. To an extent, the impact of biochar addition is reflected in the degradation and decomposition of cellulose hemicellulose structures, which are enhanced with torrefaction severity, leading to lower grinding energy. The grindability results showed lower specific grinding energy of 990.90–656.40 kJ/kg for torrefied ground SG with biochar than torrefied chopped SG with biochar (1038.90–711 kJ/kg). With an increase in torrefaction temperatures (250 °C–300 °C), the energy required for grinding decreases further from 762 kJ/kg to 656.40 kJ/kg for SG 80-20 at 250 °C/20 min and 300 °C/20 min respectively. Fig. 4 (C, D) showed the variation in the mean particle size after grinding torrefied ground or chopped SG with and without biochar.

The results demonstrated a substantial decrease in particle size, significantly affected by torrefaction temperatures. In the case of torrefied chopped SG, the mean particle size was slightly larger than that of the torrefied ground SG. Evidence of torrefaction severity embrittles the microparticle structure, reducing the strength of the cell wall, grinding efficiency and producing smaller and finer particles. Overall, the following results were achieved with biochar addition as a microwave absorber: increasing the interparticle reactivity and improving grindability. The grinding energy requirements depend on particle and sieve sizes, feed rate and biomass properties [20], and microwave absorber, as observed from the current study.

3.4. Experimental analysis and effect of the response variables

As presented in Table 2 and Fig. 4, the RSM from DOE software provided reliable fitted models, equations and correlation coefficients for response variables of torrefied SG. The response models were significant at $p < 0.05$, and the adjusted coefficient of multiple determination (R^2) was more suitable in comparing each model's adequacy (Table S2). The correlation coefficient values are closer to 1, indicating a reliable R^2 data explanation between the predicted and actual experimental values [40]. Across the R^2 predicted and R^2 adjusted values, the difference was <0.2, showing model agreement between independent and response variables. On the other hand, the coefficient of variation evaluates the experimental data's residual variation and should be <10 % [41]. Notably, the CV values agreed, resulting in the models' reliability and replicability. The multiple regression equations generated by the RSM-DOE software for each response are shown in Table S3. All models met the desirability requirement of >4, showing an adequate signal-to-noise ratio. The equations provide response interactions of SG with and without biochar torrefaction. The + represents the facilitative effect, and the – sign is the inhibitory effect; these coefficient signs in the regression equation exert facilitative (promotion) and inhibitory (suppressing) effects by influencing factors on the response value [42]. Solid yield decreased as the torrefaction temperature and residence time increased. The independent factors A, B, and C participated in the torrefaction process and reflected the inhibitory effect under a single condition. The product terms showed the same trend of inhibitory effect in AB and C^2, AC, and B^2, while C^2 showed a facilitative effect. For moisture content, B and BC (SG) and B and AC (SG-C) reflected a promotion effect, whereas other factors and product terms showed an inhibitory effect. For ash content, the influencing factor biochar had a facilitative effect under the three single factors (A, B, and C) and showed the same trend with their product terms AB, BC, and B^2 for SG and BC for SG-C. Meanwhile, AC and C^2 (SG) and AB, AC, B^2, and C^2 showed a suppressing effect. According to the regression equation, ground or chopped SG with biochar added was the most significant factor influencing the response variables. Therefore, mass yield, ash and moisture content were selected for optimal conditions to enhance solid fraction yield and future torrefied SG pellet production.

The actual and predicted values are listed in Table S4. Compared with the predicted values, the validation errors (difference in experimental data and predicted values) of solid yield, ash, and moisture (1.69 and 1.49%, 0.25 and 0.56%, and 0.06 and 0.09%) indicate satisfactory and within acceptable error of ±10% [43]. The response variables solid yield, ash and moisture contents were optimized for after-torrefaction mass yield and pelletization. The ANOVA results for torrefied ground or chopped SG indicated that the applied torrefaction conditions significantly decreased the specific grinding energy and mean particle size. Our study observed that reduced microwave energy consumption was attained at a torrefaction temperature of 250 °C (microwave power of 520 W), 20 min/20% biochar added, significantly making biochar (carbonaceous material) an adequate microwave absorber [44]. The *F*-values were highly significant at $p < 0.0001$ for all response variables, and the *p*-values were a coefficient significance check, together with the operating factor's power. The R^2 values after grinding showed little variations, 0.978 (0.906 *predicted*) and 0.995 (0.977 *predicted*) (specific grinding energy and geometer mean diameter) for torrefied ground SG and 0.977 (0.904 *predicted*) and 0.983 (0.926 *predicted*) for torrefied chopped SG. The additional advantage of microwave torrefaction is reflected in the biochar addition, which is influenced by torrefaction temperatures of 300 °C, improved crushing efficiency, and size reduction characterization for utilization in pellet production. The contour graphs for specific grinding energy analyzing the interaction effect are given in Fig. S2. The contour plots look similar in terms of understanding the interactive effect. According to the displayed graph, the trend is that higher biochar addition, higher torrefaction temperature and longer residence time resulted in lower grinding energy. Irrespective of the grinds, reduced residence time and without biochar showed higher grinding energy, as observed in the contour plot colour partition (orange-yellow-light green). Biochar addition played the most significant role in lowering the grinding energy of microwave torrefied switchgrass.

3.5. Particle surface characteristics by confocal laser scanning microscopy

Fig. 5 shows the CLSM 2D images and 2.5D display plots generated from scanning microscopy of the untreated ground (A) and

chopped (B) SG, showcasing the surface morphology variations between torrefied ground and chopped SG. The ZEN imaging software presented a collection of 2D fluorescence images observed in laser scanning microscopy (LSM 800). The imaging was transmitted into 2.5D displays, providing a detailed view of interfacial adaption and distribution of heat distortion on the microstructure surface [45, 46]. The ZEN software automatically calculated the sum fluorescence intensity (SFI) and mean fluorescence intensity (MFI), and the average SFI and MFI were compared to the untreated sample. In addition, the ZEN software 2.5D display and histogram were used to evaluate the heat penetration patterns of the microparticle surface. Untreated SG (ground or chopped) contains firm, bulky xylem tissues (Fig. 5A1 and B1). The CLSM 2.5D plots (Fig. 5A2 – A3 and B2 – B3) showed the bound fibrous structure and crack levels in ground and chopped particles, respectively, which is due to the initial handling operations. The surface morphology of each particle showcased particular evidence of surface cracks on the untreated SG before microwave torrefaction. The ground or chopped SG showed demarcated fibre-like structures, extended crack levels, and internal stacks, and they revealed the microparticle surface-size opening. Also, both SG grind particle sizes showed detailed image microparticle resolution.

The 2D images and 2.5D plots CLSM of torrefied ground and chopped SG without and with biochar showcasing surface morphology changes are presented in Figs. 6 and 7. The heating treatment method enhanced changes in the fluorescence properties of the torrefied SG structure. The imaging results validated the SEM images previously reported [37]. The untreated SG images showed significant changes compared to the torrefied SG at different torrefaction treatments. The surface microparticle plots reflected the extent of structural breakdown and computational image analysis in determining heat deformation on the surface structure at different torrefaction treatments compared to untreated SG. Fig. 6 (A1, B1), without biochar in the torrefied ground and chopped SG, revealed the impact of overheating in selected spots (hot spots) during the torrefaction reactions. The longitudinal hollow slides and fibrous stacks on images in Fig. 6(A2 and A3) represent ground SG without biochar microparticle structure produced at 250 °C/15 min residence time, and Fig. 6(B2 and B3) for chopped SG without biochar microparticle structure made at 300 °C/20 min.

The 2.5D plot displays a deep longitudinal hollow wall and fibrous gaps. The looks showed a disarranged surface, and the particle tubular structures were exposed to heat reactions at 300 °C/longer residence time/without biochar.

CLSM 2D images and 2.5D plots of microwave torrefied chopped and ground SG with biochar at torrefaction temperatures of 250 °C (Fig. 7A1 - 3) and 300 °C (Fig. 7B1 – 3). The images revealed the detailed impact of biochar addition and torrefaction reactions with variations in the torrefied SG microparticle structure and cross-sections. The 2.5 D plots showcased the changes in microparticle structure interaction with biochar addition and why the grinding performance was improved and required lower grinding energy than torrefied SG without biochar and untreated SG (Fig. 7A2 – 3, B2 – 3). The heat spreading due to the addition of a microwave absorber was more significant with torrefied ground SG/300 °C than with torrefied chopped SG/250 °C/longer residence time. However, the tubular microstructure collapsed at 300 °C/longer residence times, producing carbonized and lighter solid fractions.

Fig. 8 shows the total SFI values of torrefied ground or chopped SG compared with untreated SG. The torrefied ground SG indicated the highest SFI value at treatment levels compared to the torrefied chopped SG and untreated SG. The torrefied ground SG/10 % biochar/250 °C had the highest intensity. At the same time, the untreated SG (ground or chopped) had the lowest SFI values. SFI values denoted the total intensity of heat irradiation in the torrefied ground or chopped SG, whereas, in untreated SG, the total SFI was the result of the initial grinding and chopping process on the switchgrass surface. The heat treatment mean intensity of torrefied ground or
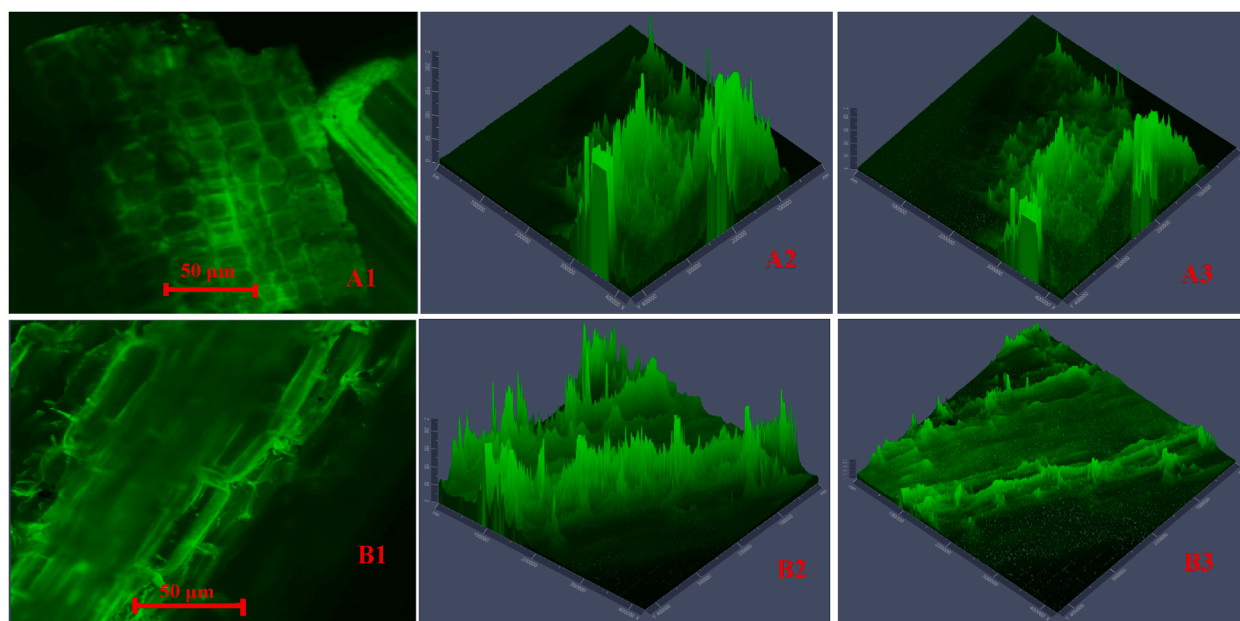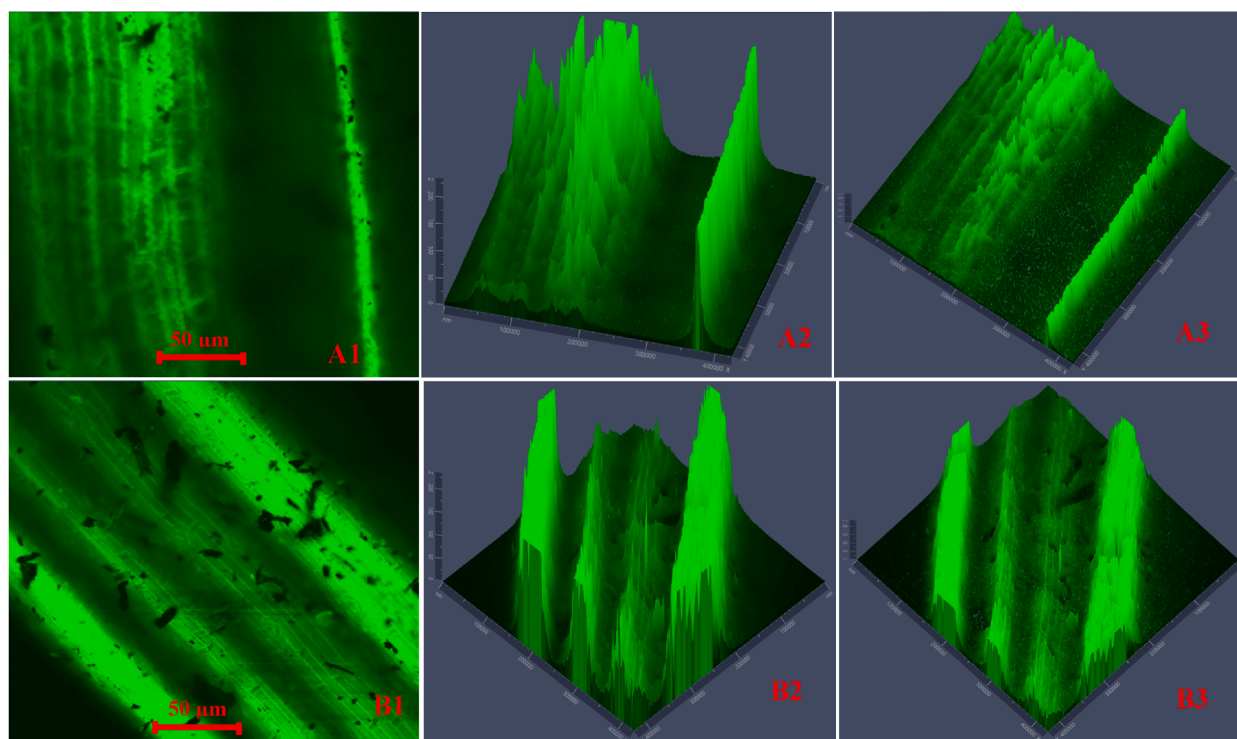

Fig. 5. Two-dimensional segmentation (A1 and B1) and 2.5D display cross-section plots (A2 – A3 and B2 – B3) for untreated ground (A) and chopped (B) switchgrass with changes in the surface morphology.

Fig. 6. 2D images (A1 and B1) and 2.5D displayed plots (A2 – A3 and B2 – B3) showing changes in fluorescence properties across surface morphology between torrefied ground (A) and chopped (B) switchgrass without biochar.

chopped SG and untreated SG are presented in Fig. 9, showcasing the MFI variations between the torrefied SG and untreated SG. The mean intensity values for torrefied ground SG/20 % biochar were greater than the torrefied chopped SG with or without biochar and untreated SG. It implies that the heat treatment effect in torrefied ground SG with biochar was responsible for the higher MFI values than in torrefied chopped SG with and without biochar.

The maximum heat deformation depth into the cell wall is presented in Fig. 10, revealing more pore spaces in torrefied ground SG than in torrefied chopped SG. The torrefied ground SG with biochar at 300 °C/longer residence times showed higher heat distortion depth. The results indicated that 20% biochar addition/250 °C created surface distortion, and torrefaction temperature at 300 °C showed colossal surface damage, producing more carbonized weight fractions. Therefore, the torrefied ground SG with biochar had higher SFI, MFI, and surface heat deformation depth than the torrefied chopped SG with and without biochar, while the untreated chopped SG without heat applied showed the lowest SFI and MFI values compared to the untreated ground SG.

## 4. Advantages of applying microwave absorbers in biomass torrefaction

The challenge of utilizing raw biomass for biofuel conversions is a major problem in storage, handling, and transportation. Biomass shows poor microwave absorption during microwave irradiation. Introducing microwave-absorptive materials has shown effective particle heat reactions in the microwave heating process and changes the thermodynamic characteristics of the irradiation process [20, 44]. The research studied the microwave torrefaction of switchgrass in two-particle sizes and biochar addition to facilitating the heating. The response of the two particle sizes with biochar shows that microwave carbon materials (biochar from forestry residues) have the absorbent qualities to convert microwave energy into heat and recycling ability for environmental sustainability. Compared with conventional methods, lower energy consumption (energy transfer instead of conventional heat transfer) is achievable with the desired product distribution (mass and energy yield) and unique particle characteristics at low torrefaction temperature and microwave power levels. The target of using microwave absorbers is to utilize less energy to produce improved solid yield and retain energy characteristics [37].

5. Conclusion

The study showcased additional techniques in characterizing microwave torrefied biomass beyond the measured physicochemical parameters. The torrefied biomass indicated the feasibility and practicality of combustion for power/heat generation or a co-burning mixture with coal. The mean particle size after torrefaction and grinding of torrefied SG decreased with increased torrefaction temperature. The grinding of torrefied ground SG with biochar resulted in lower specific energy consumption than torrefied chopped SG
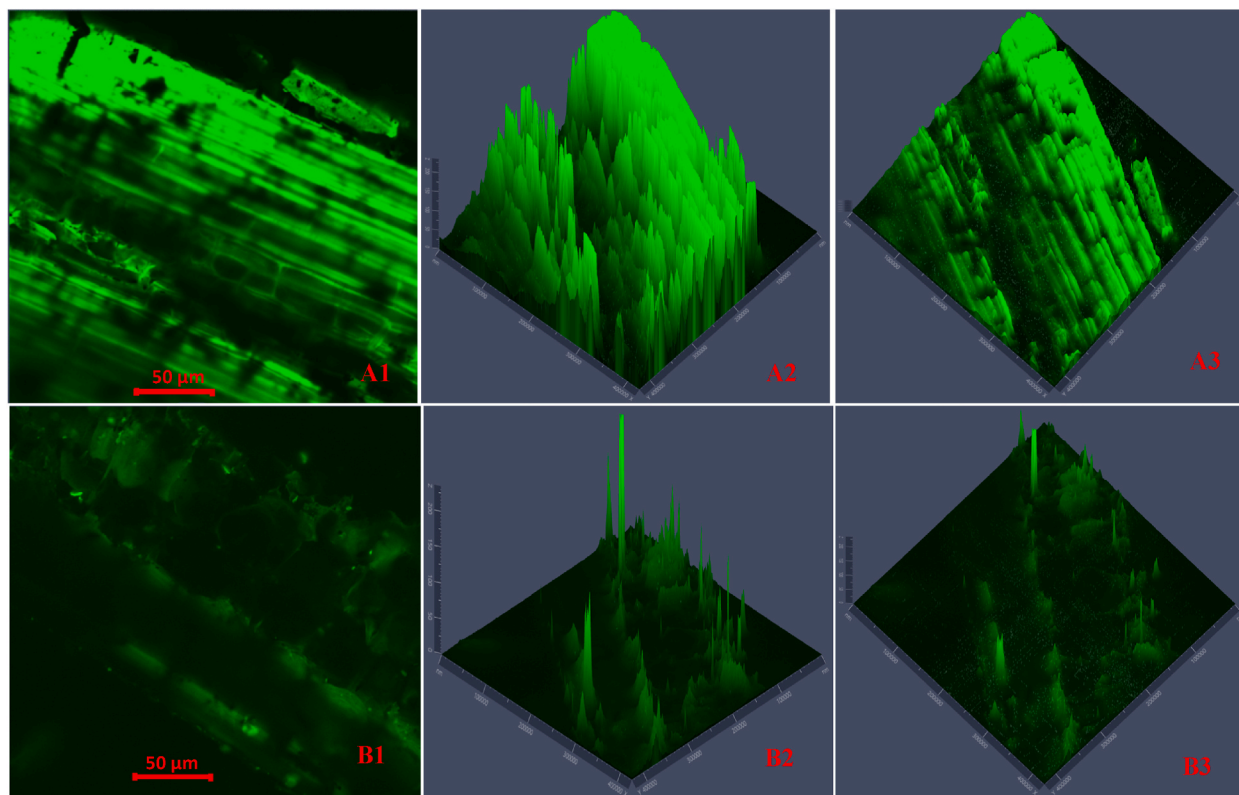
Fig. 7. 2D images (A1 and B1) and 2.5D plots (A2 – A3 and B2 – B3) showing changes in fluorescence properties across surface morphology between torrefied ground (A) and chopped (B) switchgrass with biochar.
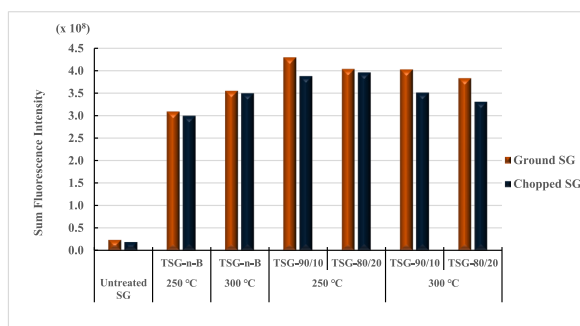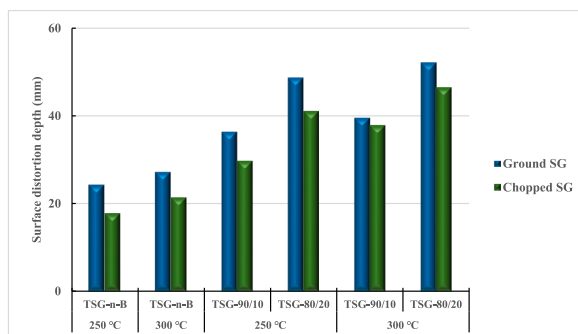

Fig. 8. Comparison of sum fluorescence intensity between torrefied and untreated switchgrass. (TSG-n-B: torrefied-switchgrass-no-biochar. The first number after torrefied biomass is % SG and the second is % biochar).

with biochar.

On the other hand, the effect of particle size depends on the torrefaction operating conditions; when the particle size diameter increases, the solid yield decreases. In addition, using a microwave absorber (biochar) in the torrefaction treatment enhanced the grindability of torrefied SG for potential utilization in fuel pellet production. The CLSM could be an alternative technique to SEM or other microscopy methods in analyzing biomass structural changes for particle size characterization and biomass densification. Furthermore, the CLSM imaging signals and 2D imaging plots indicated that adding biochar had catalyzed heating particles and the resulting microstructure of SG particles. The finding demonstrated that biochar addition greater >10%/250 °C and longer residence times showed structural alteration and, at 300 °C, caused severe colossal surface damage resulting in more carbonized weight fractions. The current study added another breakthrough in biochar application and usage, adding value to residue recycling and showcasing the potential of microwave biomass treatment technique, enhancing its readiness for commercial bioenergy applications. Furthermore, the next stage is to develop a techno-economic model, environmental impact assessment, and other potential impacts.
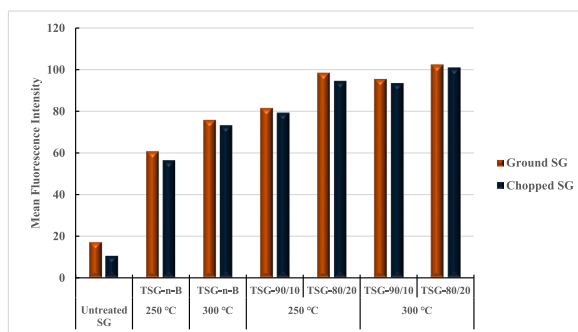
Fig. 9. Comparison of mean fluorescence intensity between torrefied and untreated switchgrass. (TSG-n-B: torrefied-switchgrass-no-biochar. The first number after torrefied biomass is % SG and the second is % biochar).

Fig. 10. Comparison of maximum penetration depth for torrefied switchgrass with and without biochar. (TSG-n-B: torrefied-switchgrass-no-biochar. The first number after torrefied biomass is % SG and the second is % biochar).

Data availability statement

Data will be made available on request.

CRediT authorship contribution statement

Obiora S. Agu: Writing – review & editing, Writing – original draft, Validation, Software, Methodology, Investigation, Formal analysis, Data curation, Conceptualization. **Lope G. Tabil:** Writing – review & editing, Supervision, Resources, Project administration, Methodology, Investigation, Funding acquisition, Data curation, Conceptualization. **Edmund Mupondwa:** Writing – review & editing, Supervision, Resources, Project administration, Funding acquisition. **Bagher Emadi:** Writing – review & editing, Methodology, Conceptualization.

Declaration of competing interest

The authors declare that they have no known competing financial interests or personal relationships that could have appeared to influence the work reported in this paper:The authors declare the following financial interests/personal relationships which may be considered as potential competing interests: Lope G. Tabil reports financial support was provided by Biofuelnet Canada. Lope G. Tabil reports financial support was provided by Natural Sciences and Engineering Research Council of Canada. If there are other authors, they declare that they have no known competing financial interests or personal relationships that could have appeared to influence the work reported in this paper.

Acknowledgments

Appendix A. Supplementary data

Supplementary data to this article can be found online at https://doi.org/10.1016/j.heliyon.2024.e32423.

References

[1] R. Font, E. Villar, M.A. Garrido, A.I. Moreno, M. Francisca, N. Ortuño, Study of the briquetting process of walnut shells for pyrolysis and combustion, Appl. Sci. 13 (2023) 6285, https://doi.org/10.3390/app13106285.

[2] P. Wang, B.H. Howard, Impact of thermal pretreatment temperatures on woody biomass chemical composition, physical properties and microstructure, Energies 11 (2018) 109–128, https://doi.org/10.3390/en11010025, 2018.

[3] O.S. Agu, L.G. Tabil, E. Mupondwa, Actualization and adoption of renewable energy usage in remote communities in Canada by 2050: a review, Energies 16 (2023) 3601, https://doi.org/10.3390/en16083601, 2023.

[4] Z. Usamni, M. Sharma, A.K. Awasthi, T. Lukk, M.G. Tuohu, L. Gong, P. Nguyen-Tri, et al., Lignocellulosic biorefineries: the current state of challenges and strategies for efficient commercialization, Renew. Sust. Energy Rev. 148 (2021) 111258, https://doi.org/10.1016/j.rser.2021.111258.

[5] F. Manzano-Agugliaro, A. Alcayde, F. Montoya, A. Zapata-Sierra, C. Gil, Scientific production of renewable energies worldwide: an overview, Renew. Sustain. Energy Rev. 18 (2013) 134–143, https://doi.org/10.1016/j.rser.2012.10.020.

[6] Y. Zheng, F. Qiu, Bioenergy in the Canadian Prairies: assessment of accessible biomass from agricultural crop residues and identification of potential biorefinery sites, Biomass Bioenergy 140 (2020) 105669, https://doi.org/10.1016/j.biombioe.2020.105669.

[7] M. Duchemin, G. Jego, R. Morissette, Simulating switchgrass aboveground biomass and production costs in eastern Canada with the integrated farm system model, Canadian J. Plant Sci. 99 (2019) 785–800, https://doi.org/10.1139/cjps-2018-0331.

[8] Agricultural Marketing Resource Center US, 2023. Switchgrass, 2023. https://www.agmrc.org/commodities-products/biomass/switchgrass. (Accessed 9 August 2023).

[9] S. Ghosh, R. Chowdhury, P. Bhattacharya, Sustainability of cereal straws for the fermentative production of second generation biofuels: a review of the efficiency and economics of biochemical pretreatment processes, Appl. Energy 198 (2017) 284–298, https://doi.org/10.1016/j.apenergy.2016.12.091.

[10] J. Whalen, C.C. Xu, F. Shen, A. Kumar, M. Eklund, J. Yan, Sustainable biofuel production from forestry, agricultural and waste biomass feedstocks, Appl. Energy 198 (2017) 281–283, https://doi.org/10.1016/j.apenergy.2017.05.079.

[11] J.H. Khalsa, D. Leistner, N. Weller, L.I. Darvell, B. Dooley, Torrefied biomass pellets—comparing grindability in different laboratory mills, Energies 9 (2016) 794, https://doi.org/10.3390/en9100794.

[12] L. Wang, L. Riva, O. Skreiberg, R. Khalil, P. Bartocci, Q. Yang, Effect of torrefaction on properties of pellets produced from woody biomass, Energy Fuel. 34 (2020) 15343–15354, https://doi.org/10.1021/acs.energyfuels.0c02671.

[13] J. Xu, Microwave Pretreatment: in Pretreatment of Biomass: Processes and Technologies, Elsevier, Waltham, MA, USA, 2015.

[14] E.T. Kostas, D. Beneroso, J.P. Robinson, The application of microwave heating in bioenergy: a review on the microwave pre-treatment and upgrading technologies for biomass, Renew. Sustain. Energy Rev. 77 (2017) 12–27, https://doi.org/10.1016/j.rser.2017.03.135.

[15] M. Wang, Y. Huang, P. Chiueh, W. Kuan, S. Lo, Microwave-induced torrefaction of rice husk and sugarcane residues, Energy 37 (2012) 177–184, https://doi.org/10.1016/j.energy.2011.11.053.

[16] S. Singh, J.P. Chakraborty, M.K. Mondal, Torrefaction of woody biomass (*Acacia nilotica*): investigation of fuel and flow properties to study its suitability as a good quality solid fuel, Renew. Energy 153 (2020) 711–724, https://doi.org/10.1016/j.renene.2020.02.037.

[17] Y. Huang, H. Sung, P. Chiueh, S. Lo, Microwave torrefaction of sewage sludge and Leucaena, J. Taiwan Inst. Chem. Eng. 70 (2017) 236–243, https://doi.org/10.1016/j.jtice.2016.10.056.

[18] A. Khelfa, F.A. Rodrigues, M. Koubaa, E. Vorobiev, Microwave-assisted pyrolysis of pine wood sawdust mixed with activated carbon for bio-oil and bio-char production, Process 8 (2020) 1437, https://doi.org/10.3390/pr8111437.

[19] S. Ethaib, R. Omar, S.M. Kamal, D.R. Awang Biak, S.L. Zubaidi, Microwave-assisted pyrolysis of biomass waste: a mini-review, Processes 8 (2020) 1190, https://doi.org/10.3390/pr8091190.

[20] J. Li, J. Dai, G. Liu, H. Zhang, Z. Gao, J. Fu, Y. He, Y. Huang, Biochar from microwave pyrolysis of biomass: a review, Biomass Bioenergy 94 (2016) 228–244, https://doi.org/10.1016/j.biombioe.2016.09.010.

[21] S.k. Satpathy, L.G. Tabil, V. Meda, S.N. Naik, R. Prasad, Torrefaction of wheat and barley straw after microwave heating, Fuel 124 (2014) 269–278, https://doi.org/10.1016/j.fuel.2014.01.102.

[22] D. Liu, N.R. Baral, L. Liang, C.D. Scown, N. Sun, Torrefaction of almond shell as a renewable agent for plastics: techno-economic analysis and comparison to bioethanol process, Environ. Res. Infrastruct. Sustain 3 (2023) 015004, https://doi.org/10.1088/2634-4505/acb5c0.

[23] X. Zheng, Z. Zhong, B. Zhang, et al., Techno-economic analysis and life cycle assessment of hydrogenation upgrading and supercritical ethanol upgrading processes based on fast pyrolysis of cornstalk for biofuel, Biomass Conv. Bioref. (2023), https://doi.org/10.1007/s13399-023-04096-x.

[24] K.L. Iroba, O. Baik, L.G. Tabil, Torrefaction of biomass from municipal solid waste fractions II: grindability characteristics, higher heating value, pelletability and moisture adsorption, Biomass Bioenergy 106 (2017) 8–20, https://doi.org/10.1016/j.biombioe.2017.08.008.

[25] S. Mani, L.G. Tabil, S. Sokhansanj, Grinding performance and physical properties of wheat and barley straws, corn stover and switchgrass, Biomass Bioenergy 27 (2004) 339–352, https://doi.org/10.1016/j.biombioe.2004.03.007.

[26] R.H. Ibrahim, L.I. Darvell, J.M. Jones, A. Williams, Physicochemical characterization of torrefied biomass, J. Anal. Appl. Pyrolysis 103 (2013) 21–30, https://doi.org/10.1016/j.jaap.2012.10.004.

[27] M. Manouchehrinejad, Y. Yue, R.A.L. de Morais, et al., Densification of thermally treated energy cane and Napier grass. Bioenerg, Res. 11 (2018) 538–550, https://doi.org/10.1007/s12155-018-9921-4.

[28] T. Melkior, S. Jacob, G. Gerbaud, S. Hediger, L. Le Pape, L. Bonnefois, M. Bardet, NMR analysis of the transformation of wood constituents by torrefaction, Fuel 92 (2012) 271–280, https://doi.org/10.1016/j.fuel.2011.06.042.

[29] J.M.C. Riberio, R. Godina, J.C. Matias, L.J.R. Nunes, Future perspectives of biomass torrefaction: review of the current state-of-the-art and research development, Sustain. Times 10 (2018) 2323. https://doi:10.3390/su10072323.

[30] Q. Bu, Y. Liu, J. Liang, H.M. Morgan, L. Yan, F. Xu, H. Mao, Microwave-assisted co-pyrolysis of microwave torrefied biomass with waste plastics using ZSM-5 as a catalyst for high quality bio-oil, J. Anal. Appl. Pyrolysis 134 (2018) 536–543, https://doi.org/10.1016/j.jaap.2018.07.021.

[31] B.A. Mohamed, C.S. Kim, N. Ellis, X. Bi, Microwave-assisted catalytic pyrolysis of switchgrass for improving bio-oil and biochar properties, Bioresour. Technol. 201 (2016) 121–132, https://doi.org/10.1016/j.biortech.2015.10.096.

[32] P.C. Hackley, A.M. Jubb, R.C. Burruss, A.E. Beaven, Fluorescence spectroscopy of ancient sedimentary organic matter via confocal laser scanning microscopy (CLSM), Int. J. Coal Geol. 223 (2020) 103445, https://doi.org/10.1016/j.coal.2020.103445.

[33] F. Depypere, P. Van Oostveldt, J. Pieters, K. Dewettinck, Quantification of microparticle coating quality by confocal laser scanning microscopy (CLSM), Eur. J. Pharm. Biopharm. 73 (2009) 179–186, https://doi.org/10.1016/j.ejpb.2009.04.007.

[34] Y. Kim, B. Kim, Y. Kim, D. Lee, S. Kim, The penetration ability of calcium silicate root canal sealers into dentinal tubules compared to conventional resin-based sealer: a confocal laser scanning microscopy study, Materials 12 (2019) 531, https://doi.org/10.3390/ma12030531.

[35] C. Maggiano, T. Dupras, M. Schultz, J. Biggerstaff, Confocal laser scanning microscopy: a flexible tool for simultaneous polarization and three-dimensional fluorescence imaging of archaeological compact bone, J. Archaeol. Sci. 36 (2009) 2392–2401, https://doi.org/10.1016/j.jas.2009.06.021.

[36] M.I. Sanhueza, R.D.P. Castillo, M. Meléndrez, C. Von Plessing, J. Tereszczuk, G. Osorio, et al., Confocal laser scanning microscopy as a novel tool of hyperspectral imaging for the localization and quantification of fluorescent active principles in pharmaceutical solid dosage forms, Microchem. J. 168 (2021) 106479, https://doi.org/10.1016/j.microc.2021.106479.

[37] O.S. Agu, L.G. Tabil, E. Mupondwa, B. Emadi, T. Dumonceaux, Impact of biochar addition in microwave torrefaction of camelina straw and switchgrass for biofuel production, Fuels 3 (2022) 588–606, https://doi.org/10.3390/fuels3040036.

[38] R. Azargohar, M. Soleimani, S. Nosran, T. Bond, C. Karunakaran, A.K. Dalai, et al., Thermo-physical characterization of torrefied fuel pellet from co-pelletization of canola hulls and meal, Ind. Crops Prod. 128 (2019) 424–435, https://doi.org/10.1016/j.indcrop.2018.11.042.

[39] M.A. Hubbe, R.P. Chandra, D. Dogu, S.T.J. Van Velzen, Analytical staining of cellulosic materials: a review, BioRes 14 (2019) 7387–7464.

[40] H. Senol, M. Ersan, F. Gorgun, Optimization of temperature and pretreatments for methane yield hazelnut shells using the response surface methodology, Fuel 271 (2020) 117585. https://doi:10.1016/j.fuel.2020.117585.

[41] S. Das, A. Bhattacharya, S. Haldar, A. Ganguly, S. Gu, Y.P. Ting, Y.P, et al., Optimization of enzymatic saccharification of water hyacinth biomass for bioethanol: comparison between artificial neural network and response surface methodology, Sust. Mater. Tech. 3 (2015) 17–28, https://doi.org/10.1016/j.susmat.2015.01.001.

[42] S. Guo, T. Guo, D. Che, H. Liu, B. Sun, Response surface analysis of energy balance and optimum condition for torrefaction of corn straw, Kor. J. Chem. Eng. 39 (2022) 1287–1298, https://doi.org/10.1007/s11814-021-1030-y.

[43] K. Kang, S. Nanda, G. Sun, L. Qiu, Y. Gu, T. Zhang, M. Zhu, R. Sun, Microwave-assisted hydrothermal carbonization of corn stalk for solid biofuel production: optimization of process parameters and characterization of hydrochar, Energy 186 (2019) 115795, https://doi.org/10.1016/j.energy.2019.07.125.

[44] M.A.H. Mohd Fuad, M.F. Hasan, F.N. Ani, Microwave torrefaction for viable fuel production: a review on theory, affecting factors, potential and challenges, Fuel 253 (2019) 512–526, https://doi.org/10.1016/j.fuel.2019.04.151.

[45] D. Song, S.E. Yang, Comparison of dentinal tubule penetration between a calcium silicate-based sealer with ultrasonic activation and an epoxy resin-based sealer: a study using confocal laser scanning microscopy, Eur. J. Dermatol. 16 (2022) 195–201, https://doi.org/10.1055/s-0041-1735429.

[46] J. Zhang, G. Zou, Y. Tan, X. Liu, G. Li, C. Zhang, Investigating the effect of preheating conditions and size effect on asphalt blending in recycled asphalt mixture: new approach based on artificial aggregate and laser scanning confocal microscopy, Construct. Build. Mater. 353 (2022) 129094, https://doi.org/10.1016/j.conbuildmat.2022.129094.